

# Hydration Disrupts Human Stratum Corneum Ultrastructure

Ronald R. Warner, Keith J. Stone,\* and Ying L. Boissy

Miami Valley Laboratories, Procter & Gamble Co., PO Box 538707, Cincinnati, OH 45253, U.S.A.; \*Winton Hill Technical Center, Procter & Gamble Co., 6300 Center Hill Avenue, Cincinnati, OH 45224, U.S.A.

**Using transmission and cryo-scanning electron microscopy, we confirm that extended water exposure leads to extensive disruption of stratum corneum intercellular lipid lamellae. We define the *in vivo* swelling behavior of the stratum corneum: exposure to water for 4 or 24 h results in a 3- or 4-fold expansion of the stratum corneum thickness, respectively. Corneocytes swell uniformly with the exception of the outermost and inner two to four corneocyte layers, which swell less. We show that hydration induces large pools of water in the intercellular space, pools that can exceed the size of water-swollen corneocytes. By 4 h of water exposure there are numerous small and large intercellular pools of water (“cisternae”) present throughout the stratum corneum, and at 24 h these cisternae substantially increase in size. Within cisternae the lipid structure is disrupted by lamellar delamination (“roll-up”). Cisternae appear to be disk-shaped structures that do not obviously**

**communicate. Cisternae appear to contain considerable lipidic and other material and to contain a substantial fluid volume that can rival the volume of the dry stratum corneum. Similar results are obtained following urine exposure. With urine exposure, cisternae communicate with salts in the external solution. This study illustrates the disruptive effect of overhydration on the stratum corneum intercellular space, identifies large and numerous unanticipated intercellular cisternal structures, defines the magnitude of stratum corneum swelling, and identifies stratum corneum cell layers that swell less. The study suggests the stratum corneum is a more chaotic structure than previously envisioned, and provides a framework for better understanding desquamation, irritancy, and percutaneous transport. *Key words: cryo/frozen hydrated/human/hydration/scanning electron microscopy/stratum corneum/transmission electron microscopy/ultrastructure/water. J Invest Dermatol 120:275–284, 2003***

It is increasingly apparent that prolonged water contact is deleterious to skin. Not only is prolonged water contact an important factor in the causation of irritant contact dermatitis (Renshaw, 1947; Suskind and Ishihara, 1965; Halkier-Sørensen *et al*, 1995), but extensive overhydration can by itself be disabling or cause intense dermatitis (Taplin *et al*, 1967; Willis, 1973; Hurkmans *et al*, 1985). Because water is known to increase skin permeability (Scheuplein, 1978), it is reasonable to link water-related dermatitis with a water-induced abrogation of the skin barrier and concomitant penetration of irritants. As the structured lipids of the stratum corneum (SC) constitute the primary permeability barrier of the skin (Onken and Moyer, 1963; Elias, 1981; Grubauer *et al*, 1989), it follows that prolonged water exposure may enhance permeation by disrupting lipid order. Recently we showed by transmission electron microscopy (TEM) that prolonged exposure of porcine skin to warm (46°C) water *in vitro* indeed caused extensive disruption of the SC lipid ultrastructure (Warner *et al*, 1999). Alterations of the intercellular lipid structure occurred after 2 h of water exposure, extensive

delamination of the intercellular lipid lamellae (lamellar “roll-up”) occurred after 6 h, and nearly complete delamination and corneocyte separation was observed after 24 h of water exposure. In human skin under ambient conditions *in vivo*, similar but less severe disruption of SC lipid ultrastructure occurred after 24 h of water exposure.

In this investigation we extend our *in vivo* studies of hydrated human SC and the lipid organization of the intercellular space. In particular we include a 4 h time point as this overhydration exposure should be similar to common human situations such as overnight diapering. We also use urine as a hydrating liquid both to compare its effects on the SC with that of water and to investigate solute entry into the SC. To overcome concerns regarding the ability of TEM sample preparation to preserve water-swollen structures faithfully, in addition to TEM we also present cryo-scanning electron microscopy (cryo-SEM) studies of frozen-hydrated samples from the same biopsies. With this latter sample preparation procedure, water remains in place, allowing direct visualization of its effect on the SC immobilized in the frozen state.

Manuscript received December 10, 2001; revised July 17, 2002; accepted for publication August 5, 2002

Reprint requests to: Ronald R. Warner, Corporate Engineering Technologies Laboratory, Procter & Gamble Co., 8256 Union Center Boulevard, West Chester, OH 54069, U.S.A. Email: warner.rr@pg.com

This work has previously been published in abstract form (*J Invest Dermatol* 110:675, 1998).

Abbreviations: TEM, Transmission electron microscopy; cryo-SEM, cryo-scanning electron microscopy; SC, stratum corneum.

## MATERIALS AND METHODS

**Tissue exposure** Subjects were two healthy male adults, ages 38 and 54. Informed consent was obtained. Hilltop patches with a chamber diameter of 19 mm (Cincinnati, OH) were saturated with distilled, deionized water, placed on the volar forearm, and sealed under occlusive tape (Durapore, 3M, St Paul, MN). The control was an untreated site from the same

forearm. After 4 and 24 h, each patch was removed and a shave biopsy quickly taken without anesthesia or other treatment. The untreated site was biopsied similarly. Each biopsy was bisected; one piece was placed in Karnovsky's fixative in 0.1 M cacodylate buffer, pH 7.4, and the other subsequently plunged into liquid ethane cooled by liquid nitrogen. The time between biopsy and freezing was less than 2 min. The frozen samples were stored under liquid nitrogen until analysis.

The same protocol was followed in concurrent studies done with Hilltop patches saturated with urine from the respective subjects.

**Transmission electron microscopy** Samples were kept in Karnovsky's fixative at 4°C overnight. The following morning the samples were cut into 1 mm cubes, rinsed in buffer, postfixed in 0.2% RuO<sub>4</sub> in 0.1 M cacodylate buffer, pH 6.8, for 1 h in the refrigerator, rinsed in buffer, dehydrated through a graded acetone series, and embedded in Spurr's resin. Thin sections were obtained and stained with uranyl acetate/lead citrate. Micrographs were obtained at 100 kV using a Philips CM12 transmission electron microscope.

**Cryo-SEM** A small ( $\approx 2$  mm  $\times$  4 mm) piece of the frozen biopsy was obtained at liquid nitrogen temperature using a precooled scalpel. Using a temperature-controlled workstation (Vestiva, Huntsville, AL), the sample was quickly mounted vertically on the slotted end of a rectangular copper block using a silver adhesive (Leitsilber 200, Ted Pella, Inc., Redding, CA) held liquid at  $-70^\circ\text{C}$ . The temperature was then lowered below  $-100^\circ\text{C}$  to solidify the adhesive. The mounted sample was transferred under liquid nitrogen to a Reichert F4CE cryo-ultramicrotome (Leica Inc., Deerfield, IL). With the sample maintained at  $-130^\circ\text{C}$ , a cross-section was planed smooth using repetitive cuts with a freshly prepared glass knife maintained at  $-120^\circ\text{C}$ . The planed sample was then mounted on a copper shuttle compatible with the cryo-stage of the Hitachi S4500 SEM and transferred under liquid nitrogen to the transfer station of the Oxford CT1500HF (Oxford Instruments, Concord, MA). From there it was transferred under vacuum to the CT1500HF workstation mounted on the Hitachi S4500 field-emission SEM (Nissei Sangyo America, Mountain View, CA). Typically, samples were etched under vacuum at  $-95^\circ\text{C}$  for up to 10 min to remove the outer surface water and reveal more of the internal ultrastructure. Samples were sputter-coated with a thin layer of gold-palladium in the Oxford workstation at  $-110^\circ\text{C}$  and transferred to the S-4500 for analysis at  $-110^\circ\text{C}$ . Analysis was usually at an accelerating voltage of 2 kV using both the upper and lower secondary electron detectors. Digital images were captured with PCI Version 5 software (Nissei Sangyo America).

X-ray analysis was performed with a rastered electron beam at 10 keV using the Link ISIS energy dispersive spectrometer (Oxford Instruments) with a Si detector and ATW window.

## RESULTS

As very similar results were obtained from the two individuals, their data were pooled.

### TEM shows that water contact *in vivo* disrupts the SC intercellular lipid lamellae and creates corneocyte separations

**Control** **Figure 1** is from an untreated control site and shows corneocytes with a normal keratin pattern and desmosomes in various stages of degeneration. The corneocytes are tightly apposed with an intercellular space of uniform dimensions and a lamellar lipid structure with a normal banding pattern (Madison *et al*, 1987; Hou *et al*, 1991).

**Four hour exposure to water** In contrast to the control, **Fig 2(a)** shows swollen corneocytes. The keratin pattern is more disorganized with frequent internal large, clear areas (presumably water). Desmosomes are less apparent. In some areas corneocytes are tightly apposed with a normal lipid lamellar banding structure (*open arrow*), but elsewhere there are frequent focal intercellular dilations (*double arrows*) containing lamellar "roll-up" (not shown) and an occasional phase-change of lipids, as shown in **Fig 2(b)**

**Twenty-four hour exposure to water** Dramatic alterations in SC morphology are observed following 24 h of water exposure, as shown in **Fig 3(a)**. Corneocytes are highly swollen and their keratin is considerably dispersed with no keratin pattern visible.

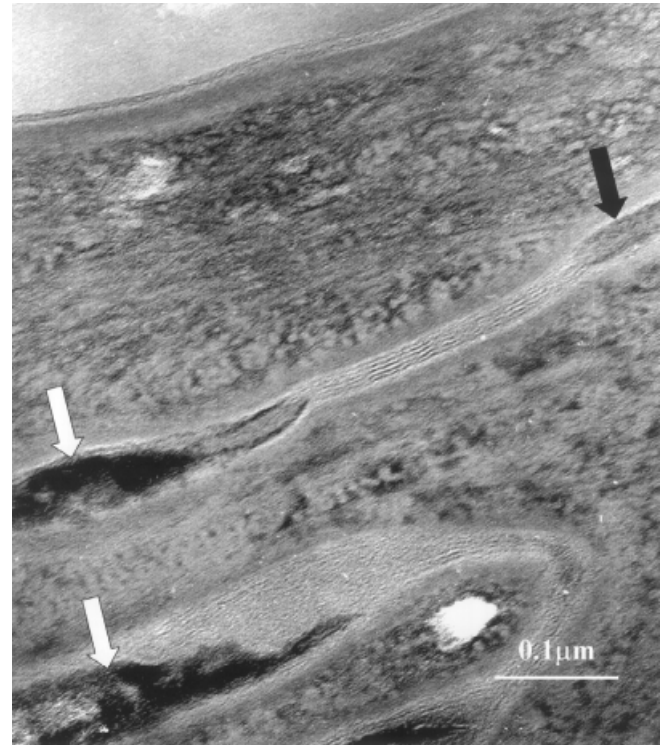


**Figure 1.** By TEM, untreated control stratum corneum has a normal morphology with tightly apposed corneocytes and a uniform intercellular space filled with lamellar lipids. The black arrow identifies a normal desmosome. Degenerating desmosomes are indicated by white arrows.

Desmosomes are rare. Although intercellular regions are still present with a normal lamellar banding pattern (*open arrow*), there are now pervasive dilations of the intercellular space. These dilations are often spindle shaped and have a spectrum of sizes from small lacunae to massive separations rivaling the thickness of the swollen corneocytes (asterisks). We have called these separations "cisternae" (Warner *et al*, 1999). The cisternae are often empty but may contain some particulate or flocculent material (*black arrow*). Intercellular lamellar lipids bordering cisternae are frequently in a disorganized state, creating a chambered appearance (*double arrows*). As shown in **Fig 3(b)**, lamellar disorganization resembling the previously described lipid "roll-up" (Warner *et al*, 1999) is also common.

### Cryo-SEM confirms that water causes SC disruption by formation of cisternae

**Control** Cryo-SEM micrographs from a control untreated site are shown in **Figs 4–6**. These images are of etched frozen tissue and have a different appearance from SEM images of dry tissue or from TEM images. Owing to the newness of this technology, a short overview of relevant morphology is presented.

**Figure 4(a)** shows a diagonal, compact SC overlying a viable epidermis that has a speckled appearance. This speckled appearance is due to small holes that likely resulted from the etching of ice crystals formed during the freezing process. There are gouges in the tissue that occurred during specimen planing. These gouges can be useful in providing three-dimensional information. In the viable tissue of **Fig 4(b)** one can easily distinguish cellular features such as nuclei and cell borders. The intercellular space has a more open, honeycomb-like structure and appears lined with smooth, homogeneous, lipid-like material.

The SC is shown at higher magnification in **Fig 5**. This is the reference image and magnification ( $\times 3000$ ) that we will use for comparison with water-exposed tissue. There are approximately 17 corneocyte layers in this image, and by comparison with the

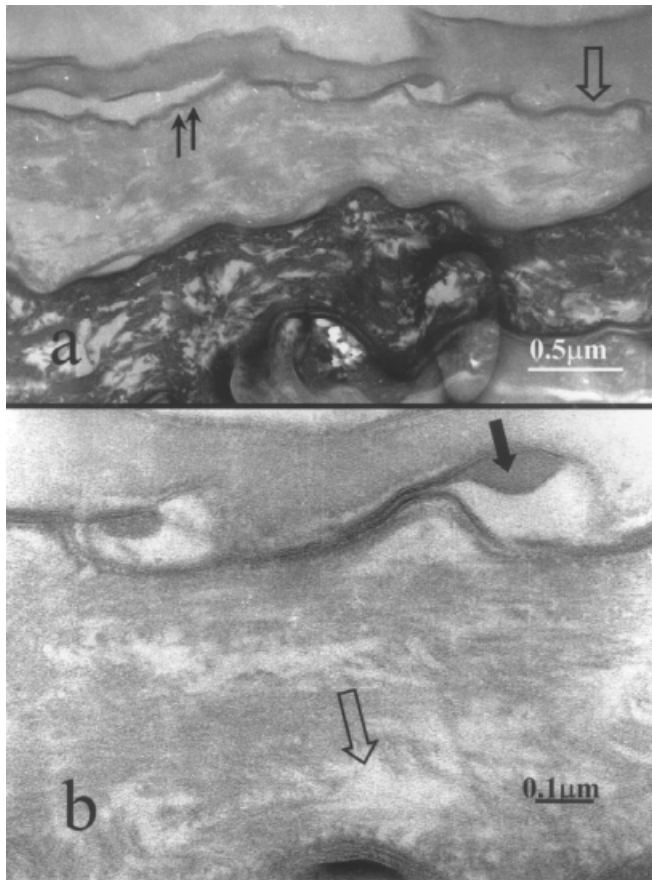


**Figure 2.** As revealed by TEM, the SC is structurally altered after exposure to water for 4 h. (a) Within the intercellular space there are areas of normal lipid lamellar structure (open arrow) juxtaposed with frequent focal dilations separating lipid bilayers (double arrows) and containing abnormal lipid structures. (b) At higher magnification focal dilations above are shown to contain amorphous lipid (black arrow). The keratin pattern is disrupted by clear areas (open arrow) that were presumably occupied by water before embedding.

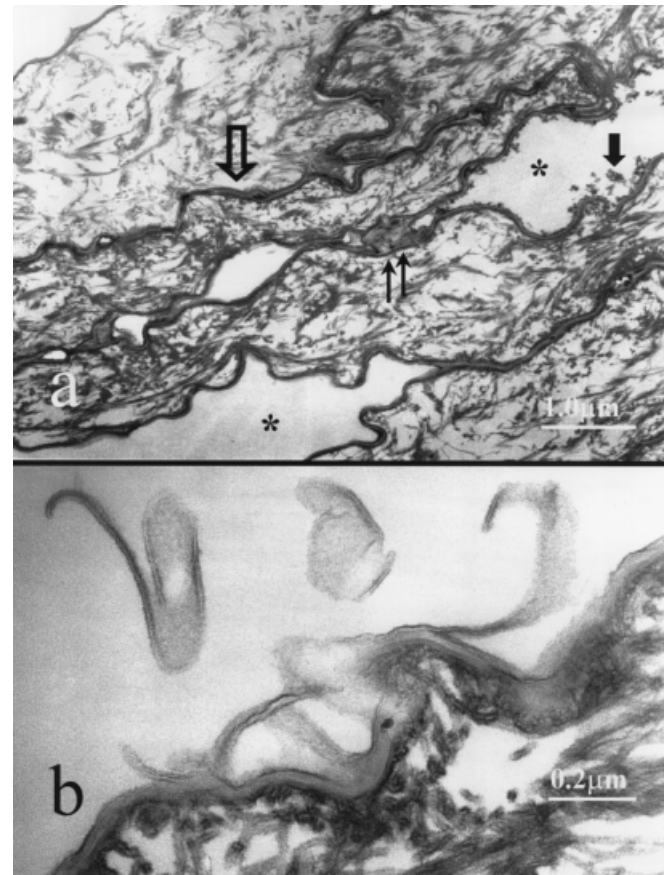


**Figure 3.** TEM reveals dramatic alterations in SC morphology following 24 h of water exposure. (a) Corneocytes are considerably swollen. Although intercellular regions containing lamellar lipids are common (open arrow), also common are very large expansions (cisternae), indicated by an asterisk. The cisternae occasionally contain flocculent material at the periphery (single black arrow). Lamellar disorganization is common (double arrows). (b) Lamellar lipid delamination or "roll up" is commonly observed within cisternae.

lower-right scale bar, the SC is slightly greater than 10  $\mu\text{m}$  thick. The corneocytes are tightly apposed; separations are minimal. In the upper granular layer, spherical structures similar to lamellar bodies are evident within the keratinocytes.

**Figure 6(a)** shows SC structure at a "gouge" region with three-dimensional features. The internal corneocyte structure is compact and massively filled with material (open arrow) having a structure consistent with the keratin pattern of **Fig 1**. Unlike the viable tissue, there are few holes formed from etched ice crystals, indicating lower water content, higher freezing rates, or both. Lipid lamellar bilayers are readily visualized in cross-fractures across the intercellular space (black arrow). The lamellar lipid surfaces form smooth and homogeneous sheets. Occasional protruding half-micron circular structures (double arrows) have not been unequivocally identified, nor were desmosomes recognized. As shown in **Fig 6(b)**, occasional vacuolar "pockets" are present in the intercellular space (arrows). These pockets are empty in this etched sample but may have contained water. Similar structures can be observed in **Fig 5** (arrow).

**Four hour exposure to water or urine** An overview of water-exposed tissue is shown in **Fig 7**. The tissue morphology is similar following urine exposure. The SC thickness (white arrows) is greatly increased over the control (compare with **Fig 4a**). The individual corneocytes appear approximately equivalently swollen throughout with the exception of the outermost and innermost few

corneocytes. Multiple samples from biopsies of both subjects exhibited this effect. The SC is no longer homogeneous in appearance but contains focal regions of more deeply etched tissue (black arrows).

As shown at the higher (reference) magnification in **Fig 8**, the SC thickness has increased 3-fold to about 30  $\mu\text{m}$  and now occupies nearly the entire field of view; contrast this image with **Fig 5**. The swollen corneocytes have a lattice of keratin filaments similar to the TEM images at this time point (**Fig 2**). The relative homogeneity in swelling of the corneocytes is readily seen, as is the lack of participation in this swelling by the outermost few corneocyte layers (lower left corner of **Fig 8**) and the more dense, bright-appearing innermost few corneocyte layers.

In addition to corneocyte swelling, water also appears within the intercellular space in the form of discrete regions of localized swelling. Small dilations of the intercellular region are common and easily seen throughout the SC (small arrows of **Fig 8**). Larger dilations are also present, typically near the SC surface (large arrows). These large distensions can exceed the size of swollen corneocytes, and would thus appear to be similar to the cisternae seen in the TEM images (**Fig 3**). Intercellular dilations of any size were very rarely found within the inner (less swollen) SC.

Cisternae are not empty but contain substantial amounts of nonkeratin-appearing material with diverse structures. Examples of the morphology of cisternae under both etched and hydrated conditions are shown in **Fig 9**. We believe **Fig 9(d)** shows the

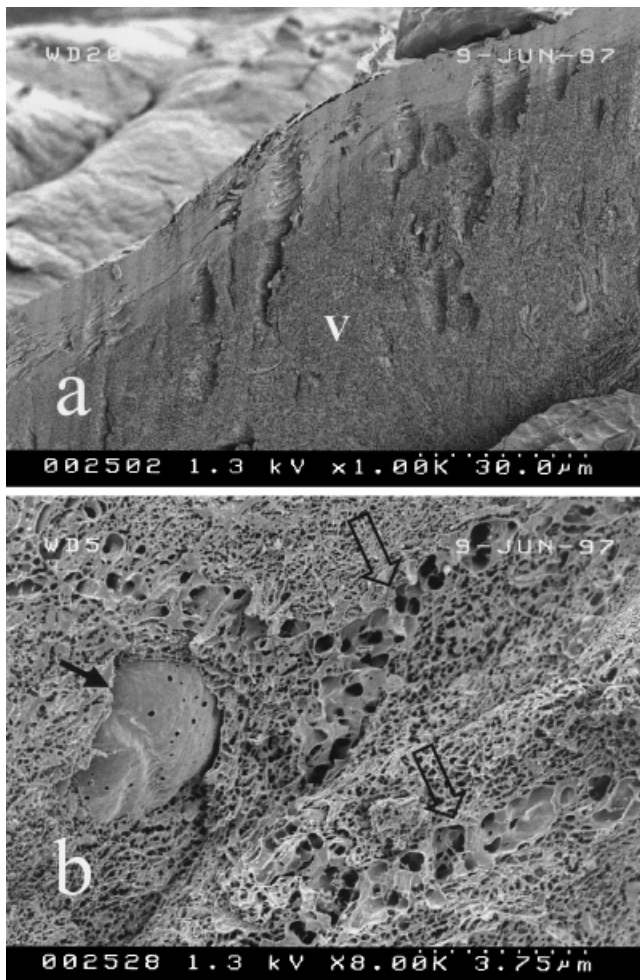


**Figure 4.** (a) This Cryo-SEM micrograph of control untreated skin is divided by a transverse band of homogeneous-appearing SC consisting of tightly apposed corneocytes overlying a more varied viable epithelium. The (out-of-focus) surface of the skin is in the upper left of the image, the viable epithelium in the lower right ("V"); the 30  $\mu\text{m}$  magnification bar on the bottom right of the micrograph encompasses the total width of the 11 equidistant dots. (b) The viable tissue at higher magnification reveals cellular cytoplasm with submicron ice crystal damage and morphologic structures such as nuclei (black arrow) and the intercellular space (open arrows).

three-dimensional shape of a cisterna. The fracture plane reveals a lipid-enclosed, limited, apparently disk-shaped structure (open arrow) within the ordered array of linear corneocytes.

*Twenty-four hour exposure to water or urine* An overview of water-exposed tissue is shown in **Fig 10**. The tissue morphology is similar following urine exposure. This specimen is minimally etched and water (ice) remains in contact with the SC surface. Similar to the TEM observations, with further time of water contact the SC continues to swell; from the scale bar, the SC is now approximately 40  $\mu\text{m}$  in thickness. Similar to the 4 h exposure, the corneocytes are approximately equivalently swollen throughout with the exception of the innermost few corneocytes that swell less than their more mature counterparts, and the very outermost corneocyte layer, which is little changed from its control corneocyte thickness. The lack of swelling of the outermost corneocyte layer is particularly perplexing as this outermost corneocyte "scale" is completely surrounded by external water at the skin surface.

As shown in **Fig 11** at the reference magnification of  $\times 3000$ , the SC can now no longer be contained within a single image;



**Figure 5.** Cryo-SEM of control, untreated SC at a reference magnification of  $\times 3000$  shows an approximately 10  $\mu\text{m}$  thick structure of tightly apposed corneocytes with minimal intercellular space. Occasional vacuolar structures are present (arrow). Thin linear separations between corneocytes may be artifacts of the cryo-planing process.

**Fig 11** is a composite of two micrographs. The increase in SC thickness is in part due to increased corneocyte hydration, the corneocyte thickness increasing 30–50% *vs* the 4 h time point. The keratin filaments within corneocytes form a more open network similar to the TEM observations (**Fig 3**). The other contributor to SC thickness, and again similar to TEM observations, are the numerous large water-filled distensions of the intercellular space (cisternae), identified by an asterisk in **Fig 11**. These cisternae are now easily recognized by their spindle shape, by the slight depression of their surface below the corneocyte level due to a slight etching, but in particular by the absence of keratin filaments and instead an internal morphology of sparse planar/globular structures within an ice matrix.

The size of these cisternae is considerably enhanced over the 4 h time point (**Fig 8**).

**Do cisternae intercommunicate?** Of interest is whether cisternae communicate, providing a continuous water path across the SC. There are no obvious water-filled intercellular channels connecting cisternae, as indicated in **Figs 11** and **12**. The intercellular spaces between cisternae typically appear sealed over most of their length.

Further, in a fortuitous fracture the fluid content of a cisterna can be seen to terminate, as shown in **Fig 13**. This micrograph shows a lamellar surface of the intercellular space, and to the right the fluid content of a cisterna (containing globular material). Between them can be seen a clear border or termination of the fluid droplet that presumably penetrates between lipid bilayer leaflets.

Whereas this would strongly argue that some if not all cisternae are bounded and not in continuous contact across the SC, we have occasionally found evidence to the contrary, as shown in **Fig 14** from urine-exposed tissue in which the solid arrow points to what could be a patent intercellular space connecting cisternae. This image also shows very rare dilations of the intercellular space in the inner SC (open arrows).

**Cisternae can be large** Typically there is a gradient in size of cisternae across the SC. The largest cisternae are near the SC surface and can be remarkably large, as illustrated in **Fig 15**. The outer cisterna in this micrograph is nearly 15  $\mu\text{m}$  high, a thickness greater than that of the entire SC prior to water exposure! Cisternae (and therefore the intercellular space) occupy a substantial fraction of the SC volume following extended water

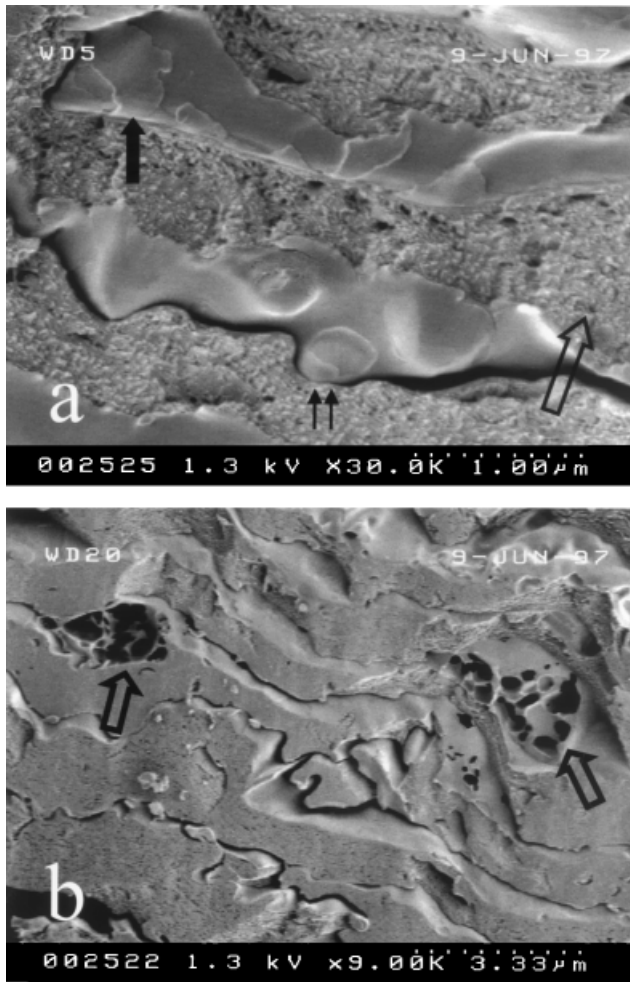


**Figure 6. Higher magnification of control SC reveals corneocyte internal structure, intercellular lipid lamellae, and occasional intercellular vacuolar "pockets":** (a) This image is from a "gouge" region (cryo-fracture). The three-dimensional structure shows three corneocyte "steps" that are descending from the image top to the bottom. The two "risers" separating the three corneocytes are the intercellular spaces, which are filled with a smooth-surfaced material that is lamellar in nature (*black arrow*) and therefore corresponds to lamellar lipids. (b) Occasional intercellular spaces appear widened with a possibly chambered lipid structure (*open arrows*). The holes in these lipid membranes may be artifacts of the etching process.

exposure. The intercellular space alone can rival the volume of the dry SC.

**Cisternae contain solutes from the external fluid** As shown in **Fig 16(a)**, the X-ray spectrum reveals small peaks for Na, Cl, and K within an outer cisterna of urine-exposed skin. The Au and Pd peaks are from the conductive coating sputtered on the sample surface. The small peaks for the physiologic elements are less an indication of quantitatively small concentrations than they are the poor analytical sensitivity of this technique under the X-ray absorbing conditions of a metal coating and full hydration. For instance, physiologic elements were not detected in the viable epidermis! We are only measuring very elevated levels of these physiologic elements; however, these elements from the external fluid were detected in the urine-treated SC. In this tissue, the amount of Na and Cl within cisternae decreases with depth into the SC (data not shown). Within corneocytes, Na and Cl are present but at lower concentrations (**Fig 16b**). No or much reduced levels of Na and Cl are present in water-exposed skin (outer cisternae, **Fig 16c**).



**Figure 7. Cryo-SEM of skin exposed to water for 4 h shows a considerably expanded SC with focal disruption of the intercellular space.** The SC thickness (noted by *white arrows*) is considerably swollen; compare with **Fig 4(a)** at the same magnification. Within the SC are occasional spindle-shaped expansions of the intercellular space (*black arrows*) that are more prevalent near the SC surface.



**Figure 8. At the reference magnification, the SC has swollen 3-fold following 4 h of water exposure.** The SC outer surface is at the lower left-hand corner. Dilations of the intercellular space are common. Small dilations (*small arrows*) present an appearance of "ponds" being fed by intercellular "tributaries". Larger dilations (*large arrows*) are typically close to the SC surface. The cisternae contain considerable collapsed internal material in this etched tissue.

## DISCUSSION

**Water disrupts SC structure** It is known that water increases the permeability of skin (Fritsch and Stoughton, 1963; Scheuplein, 1978; Zimmerer *et al*, 1986). The mechanism by which water elicits this change is not known, nor is the relationship between permeability and the extent of overhydration (Zhai *et al*, 2001). In this paper we show that extended water contact disrupts the lipid lamellar architecture of the intercellular space, which may be the cause of the increased SC permeability.

Previously we showed by TEM that exposure of porcine skin to warm water *in vitro* for several hours resulted in a dramatic disruption of SC lipid organization (Warner *et al*, 1999),

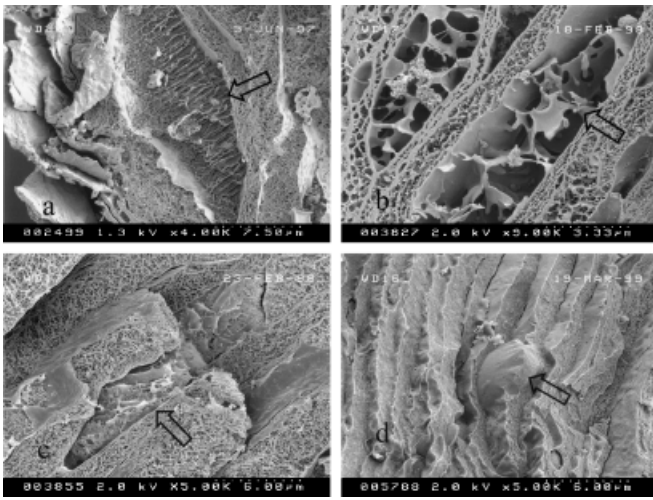


**Figure 9.** Cisternae present various internal morphologies and appear limited in size. These micrographs are from different preparations under different etching conditions; magnifications vary. Owing to the nature of the freezing and etching process, and possible contamination of surfaces with planing debris or “dirty” liquid nitrogen (specimen transfer), there is ample opportunity for artifacts to be present in these images of presumably dilute intercellular solutions within cisternae. Clearly the internal structures differ from keratinocytes; there is a recessed visible ice floor, an absence of keratin filaments, and the presence of globular/particulate structures and planar lipid-like membranes. (a) Four hour water exposure. A large cisterna near the SC surface has unusual vertically oriented planar structures (*open arrow*). (b) Four hour water exposure. A deeply etched cisterna has a chambered appearance of lipid-like membranes (*open arrow*). These membranes are continuous with the lamellar cisternal walls, and may represent the lipid “roll-up” seen in TEM images (Fig 3). (c) Twenty-four hour water exposure. The three-dimensional nature of cisternae is apparent, with lipid-like membranes in a water matrix (*open arrow*). (d) Four hour urine exposure. Approximately 14 corneocyte layers are shown, with an apparent intercellular lipid-enclosed cisterna mid-way within the SC (*open arrow*). The cisterna is disk-shaped similar to that suggested by c.

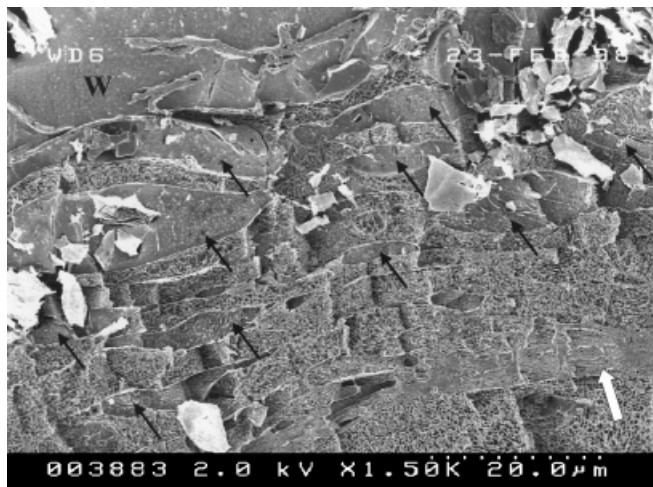


**Figure 10.** Cryo-SEM of skin exposed to water for 24 h shows a continued expansion of the SC with increased focal disruption of the intercellular space. In spite of the considerable debris on the cut surface, it is easy to identify the many cisternae filled with water (*black arrows*). External water remains on the skin surface (“W”). The innermost corneocytes are poorly swollen (*white arrow*).

characterized by large separations between corneocytes and delamination of the intercellular lamellar lipids within this presumed water phase of the SC. We showed similar effects *in vivo* in human skin exposed to water at ambient temperature. In



**Figure 11.** At the reference magnification, a composite of two micrographs shows the SC expanded to a thickness of approximately 40  $\mu\text{m}$  following 24 h of water exposure. The increase in thickness is due to the increased swelling of corneocytes and to a considerably enhanced size of cisternae, indicated by an asterisk. The SC surface is just above the top of this image.

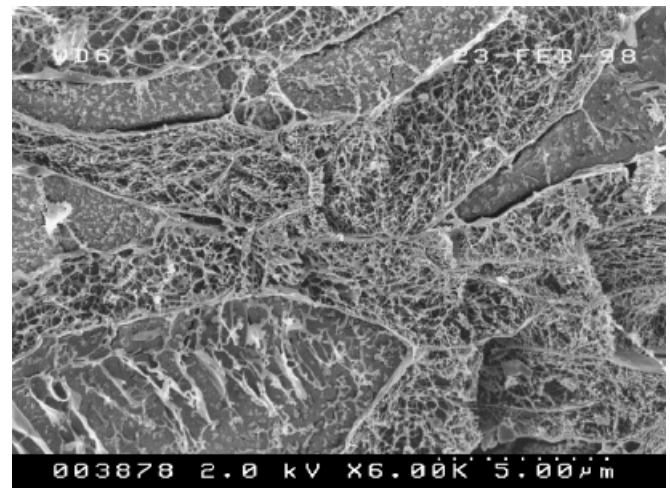


**Figure 12.** There is no obvious open channel of intercellular fluid between cisternae. At least visually, cisternae appear to be isolated structures that do not intercommunicate. This image is from skin exposed to water for 24 h.

this paper we used two different morphologic techniques, TEM and Cryo-SEM, to confirm a disruptive effect of extended hydration on human SC lipid structure *in vivo*. After just 4 h of water exposure the SC is dramatically expanded to three times its normal thickness, increasing to 4-fold by 24 h. This expansion



**Figure 13.** Fluid within cisternae appears to terminate with defined borders. Cisternal fluid in this image terminates as a thinned layer demonstrating sized-excluded particulates. This image is from skin exposed to water for 24 h.

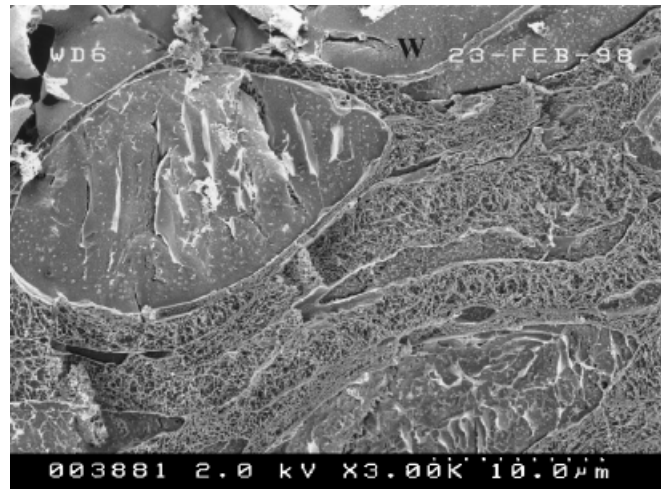


**Figure 15.** Cisternae tend to be larger near the surface and individually can have heights exceeding the thickness of the control SC. In this image from skin exposed to water for 24 h, the outer cisterna height is nearly 15 µm. Compare this single cisterna with the SC of Fig 5, obtained at the same magnification.

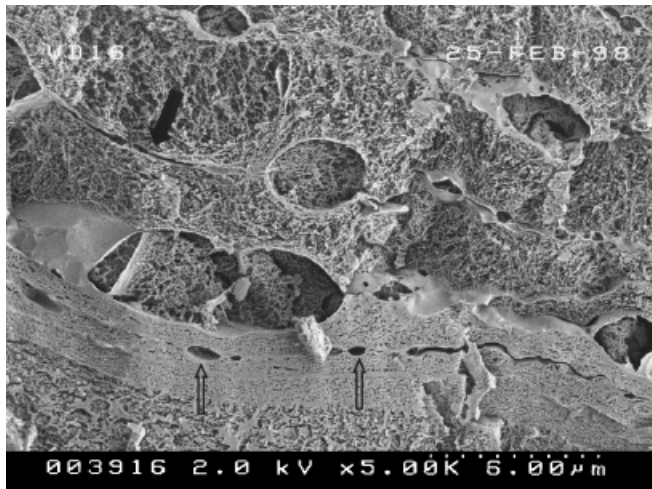


**Figure 14.** Visibly communicating cisternae are rare; however, occasionally an intercellular space appears to be relatively continuously open between cisternae (black arrow), as shown in this tissue exposed to urine for 24 h. Very rare dilations in the inner SC are indicated by open arrows.

occurs due to water uptake by corneocytes, which proceeds nearly uniformly across the SC, and occurs due to substantial water imbibition within the intercellular space in discrete foci or cisternae. The cisternae dramatically increase in size and number across the SC as a function of time. The lamellar lipid delamination that occurs within cisternae, as visualized by TEM, is presumably due to water destabilization of lamellar structure. As discussed previously (Warner *et al*, 1999), the intercellular lipid bilayer structure of human SC does not appear to be constructed for extended water contact and is but a temporary barrier against prolonged water exposure. Extended water contact, such as that encountered by marine mammals or occurring within the oral mucosa, requires a different barrier structure (Menon *et al*, 1986; Elias and Menon, 1991; Law *et al*, 1995).

The existence of large water-filled structures (cisternae) within the SC is surprising but supported by the literature. The ability of the SC to imbibe copious quantities of water is well documented (Scheuplein and Morgan, 1967; Spencer *et al*, 1975). The presence of cisternae within the SC is supported by a freeze-fracture study

of isolated human SC hydrated in buffer for 48 h, which reported numerous “water pools” within the SC intercellular space (van Hal *et al*, 1996). Previous studies using more conventional microscopy techniques had also reported that hydration caused formation of large intercellular clefts in the SC (Agache *et al*, 1973; Kligman, 1994). Although these earlier studies support our findings, none of them effectively communicated the extensive disarray of the SC barrier and the massive amount of imbibed fluid that occurs with overhydration.

Corneocyte swelling can be readily understood in terms of water moving intracellularly in response to osmotic gradients. The existence of cisternae within the intercellular space is harder to explain. The focal nature of cisternae could suggest there is a focal distribution of solutes within the SC intercellular space. One source of solutes could be the breakdown of corneodesmosomes, known to occur in a graded fashion across the SC (Chapman and Walsh, 1990; Fartasch *et al*, 1993). Indeed, dilations of the intercellular space at sites of corneodesmosome dissolution have been observed previously in murine skin following microwave fixation and under a variety of conditions that enhance percutaneous transport (Menon and Elias, 1997). Corneodesmosome degradation is known to be a function of water content (Rawlings *et al*, 1995; Koyama *et al*, 1997), and both a previous study (Warner *et al*, 1999) and this study observed fewer corneodesmosomes as a function of water exposure. In this scenario, with increasing water influx into the SC there is increasing corneodesmosome degradation and increasing focal production of osmotic solutes, leading to an ever-increasing number and size of cisternae. We believe the enormous size of some cisternae and the presence of apparently copious quantities of material within them argue for solute contributions from additional sources, such as the leaching of osmolytes from corneocytes. This hypothesis is supported by a recent study observing distended lacunae at presumably noncorneodesmosome sites in SC exposed to agents that enhance permeation (Jiang *et al*, 2000).

**The effect of urine is similar to that of water** We thought that urine exposure would result in less swelling of the SC due to osmotic effects. If differences in swelling did exist, they were not obvious. A tentative conclusion would be that the osmolarity of the urine was small compared with the natural osmolarity of the *in vivo* SC. One difference in urine-exposed SC was that cisternae appeared to contain more planar structures similar to

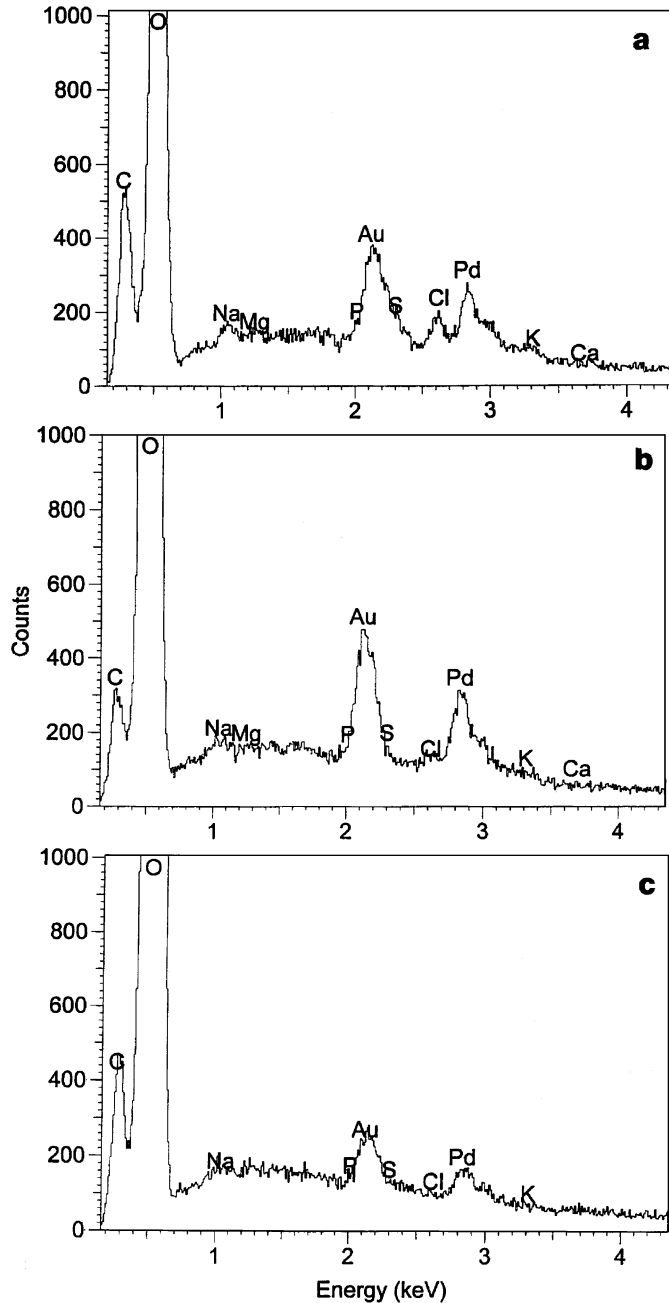


**Figure 16.** Cisternae from urine-exposed skin contain the urinary elements Na, Cl and K; cisternae from water-exposed skin do not. (a) Spectrum from an outer cisterna of urine-exposed skin. The Au and Pd peaks are from the sputtered coating. (b) Spectrum from a mid-level corneocyte of urine-exposed skin. (c) Spectrum from an outer cisterna of water-exposed skin.

those shown in Fig 9(a) (but with the planar structures running in diverse directions). These structures were particularly evident in larger cisternae near the SC surface. We believe the planar structures are artifacts attributed to the freezing of a largely unstructured water phase. Their abundance in urine-exposed tissue, however, suggests that there were more (urine-derived) solutes in these cisternae, as supported by Fig 16.

**Swelling of the SC *in vivo* is similar to that *in vitro*** To the best of our knowledge we believe our study is one of the first quantifications of SC swelling *in vivo*. The magnitude of SC swelling *in vitro* is controversial (Scheuplein and Morgan, 1967; Norlén *et al*, 1997). The increase in SC thickness that we observe

*in vivo* is in reasonable agreement with previous calculations of isolated SC thickness following hydration *in vitro* (Scheuplein and Morgan, 1967). In this latter study, hydration for 5 h resulted in a 2.6-fold expansion, comparing well with our estimated 3-fold value at 4 h, and hydration for 25 h resulted in a 3.8-fold expansion, comparing well with our estimated 4-fold value. If we assume that this *in vivo/in vitro* correlation were to continue for longer exposure times, then we would predict that the *in vivo* SC would continue to expand to approximately 4.5-fold times its original thickness over an additional 1 or 2 d (Scheuplein and Morgan, 1967). This implies that the 24 h time point that we observe is not fully expanded, but is nearly so.

**Do outermost corneocytes lack osmolytes?** The outermost corneocytes apparently do not significantly imbibe water. Although we cannot rule out a dry-down (desiccation) artifact that occurred prior to freezing, we have observed surface water in contact with outer corneocytes that were not swollen, arguing against this possibility. Outer corneocytes may have simply lost extensibility. Alternatively, the outer corneocytes may have lost their internal osmolyte contents as suggested by precipitous drops in the concentration of natural moisturizing factors in the uppermost part of the SC (Caspers *et al*, 2001). The apparent different interaction of the outermost layer with water suggests corneocyte property changes that could be involved in the ultimate step of desquamation.

**Are innermost corneocytes a barrier?** As shown in this investigation, the innermost two to four corneocytes strikingly imbibe considerably less water than the bulk of the SC. Furthermore, cisternae are not found in this region following water-only exposure. One explanation is that there is less force for water uptake (fewer osmolytes) in this region. The source of osmolytes within corneocytes must in part be due to the breakdown of filaggrin into natural moisturizing factors (Scott *et al*, 1982), which occurs over the inner SC (Steven *et al*, 1990). The innermost SC would thus not have the full complement of osmolytes, an explanation supported by previous observations that the lower layers of the SC have a lower water-holding capacity, a lower level of extractable amino acids (Hashimoto-Kumasaka *et al*, 1991), and a sharp drop in natural moisturizing factors (Caspers *et al*, 2001). Alternatively, the structural presence of filaggrin may simply limit the extensibility of the innermost corneocytes.

The location of the "skin barrier" within the epithelium has been debated for decades (Blank, 1952; Matoltsy *et al*, 1968; Bowser and White, 1985), and current thinking suggests this barrier resides in the lipids (Elias, 1981; Grubauer *et al*, 1989), the fluid domains of those lipids (Barry, 1988; Forslind, 1994; Bouwstra *et al*, 2000), and the tortuous path of the totality of the SC intercellular space (Potts and Francoeur, 1991; Johnson *et al*, 1997). We are seeing that the innermost corneocytes are a distinctly different compartment from the remainder of the SC, however, differing in terms of elemental ionic composition (Warner *et al*, 1995), lipid composition (Lampe *et al*, 1983), natural moisturizing factor constituents (Caspers *et al*, 2001), equilibrium water binding capacity (Hashimoto-Kumasaka *et al*, 1991; Warner and Lilly, 1994), and now swelling behavior. With extended water exposure the lipid lamellae of this region do not participate in cisternae formation. As this inner SC intercellular space is the region over which lipid lamellae are being formed, and the intercellular lipids of these inner layers have a composition and structure different from the remainder of the SC (Lampe *et al*, 1983; Madison *et al*, 1987; Elias *et al*, 1988), it is thus not too surprising that this intercellular space may function differently. If the SC barrier resides in intercellular lipid lamellae and long diffusional path lengths, this barrier likely extends down to the innermost SC but may not include it, the innermost SC being a different barrier. In this regard, the presence of glycolipids in this inner region (Lampe *et al*, 1983) is similar to their presence in the oral mucosa (Squier *et al*, 1991) and in the skin barrier of marine



mammals (Menon *et al*, 1986). Although the role of glucosylceramides in marine SC or oral mucosa is not understood, if they are a barrier in these tissues they could represent an equivalent barrier in the lower SC. Certainly the images of the inner SC such as those of **Fig 11** and **14** suggest this layer has the structural potential to have barrier properties. The question is whether imbibed water readily passes through these inner layers leaving them unswollen, or whether water ingress is impeded by these layers, leaving them unswollen.

**What is the effect of cisternae on SC function?** Our observation of cisternae within the SC is a challenge to the understanding of SC function. What are these structures, and what part might they play? As cisternae appear to contain solutes (NaCl) from the external (urine) solution, they could be involved in permeation. Equally pertinent could be the fate of external solutes within cisternae following "dry-down". The loss of imbibed water during dry-down may occur without the equivalent removal of permeating solutes, leaving them trapped within the newly reformed SC intercellular spaces and creating a "reservoir" within the SC (Vickers, 1963). Although we have not studied dry-down, the vacuolar "pockets" that we commonly observe in control SC (**Figs 5** and **6b**) are similar to cisternae, suggesting that pockets of fluid may commonly reside within the normal SC. Pockets of fluid or cisternae may not be static within the SC (Menon and Elias, 1997), suggesting the SC may have a more chaotic structure than the brick wall (Michaels *et al*, 1975) or domain mosaic model (Forslind, 1994) previously envisioned.

**Implications for occupational dermatology** Our confirmation that water disrupts the structure of the SC barrier lipids helps explain the known ability of water to increase skin permeability (Scheuplein, 1978). Similarly, our results strongly support the ability of prolonged water contact to facilitate irritant contact dermatitis (Renshaw, 1947; Suskind and Ishihara, 1965; Possick, 1969; Halkier-Sørensen *et al*, 1995; Meding, 2000). The reputation that water is innocuous comes from innumerable studies that show occluded patch exposure using water does not result in visible erythema even after days of exposure (e.g., Basketter *et al*, 1998). Indeed, in our study, skin that was patched with water or urine for 24 h had no observable erythema; however, our results show that the absence of erythema does not imply an absence of damage. This observation is consistent with the literature, where continuous exposure to water or occlusion for 6–48 h resulted in keratinocyte vacuolization and changes in Langerhans and mononuclear cells, but no reported dermatitis (Jolly and Swan, 1980; Lindberg and Forslind, 1981; Lindberg *et al*, 1982; Mikulowska, 1990, 1992; Kligman, 1994). With water exposure in excess of a few days, visible dermatitis is observed (Taplin *et al*, 1967; Willis, 1973; Kligman, 1994). It has been suggested that prolonged water exposure could result in cumulative damage to the SC, resulting in sufficient water entry into the viable tissue to exert cytotoxic effects directly (Willis, 1973). This mechanism may also apply to surfactant-induced irritation, as surfactants increase water permeation across skin (Bettley and Donoghue, 1960). Surfactant-induced irritation could be due, at least in part, to an enhanced rate of water entry into the viable tissue, decreasing the time needed to create visible water-induced dermatitis (Warner *et al*, 1999). Alternatively, it has been proposed that water is a facilitating rather than a causative agent; a water-induced increase in SC permeability would promote the delivery of potential irritants (Suskind and Ishihara, 1965). Similar to our observations on urine salts within cisternae, it is possible that large amounts of irritants could become incorporated within the SC during a swelling phase, and repeated swelling events on a regular basis might result in greatly enhanced transdermal delivery of this "preloaded" SC. In support of this concept, transdermal delivery for many compounds correlates directly with the amount incorporated within the SC (Rougier *et al*, 1985). To the extent that SC is an

accordion-like structure during swelling and drying events, it may also be an imbibing structure resulting in extended contact with internalized solutes that could play a part in irritancy.

---

*R. Warner dedicates this paper to Albert Kligman, who has been an inspiration and an important source of encouragement.*

---

## REFERENCES

- Agache P, Boyer JP, Laurent R: Biomechanical properties and microscopic morphology of human stratum corneum incubated on a wet pad in vitro. *Arch Derm Forsch* 246:271–283, 1973
- Barry BW: Action of skin penetration enhancers—the lipid protein partitioning theory. *Int J Cosmet Sci* 10:281–293, 1988
- Basketter D, Gilpin G, Kuhn M, Lawrence D, Reynolds F, Whittle E: Patch tests versus use tests in skin irritation risk assessment. *Contact Dermatitis* 39:252–256, 1998
- Bettley FR, Donoghue E: Effect of soap on the diffusion of water through isolated human epidermis. *Nature* 185:17–20, 1960
- Blank IH: Factors which influence the water content of the stratum corneum. *J Invest Dermatol* 18:433–440, 1952
- Bouwstra JA, Dubbelaar FER, Gooris GS, Ponc M: The lipid organization in the skin barrier. *Acta Derm Venerol* 208:23–30, 2000
- Bowser PA, White RJ: Isolation, barrier properties and lipid analysis of stratum compactum, a discrete region of the stratum corneum. *Br J Dermatol* 112:1–14, 1985
- Caspers PJ, Lucassen GW, Carter EA, Bruining HA, Puppels GJ: *In vivo* confocal raman microspectroscopy of the skin: noninvasive determination of molecular concentration profiles. *J Invest Dermatol* 116:434–442, 2001
- Chapman SJ, Walsh A: Desmosomes, corneosomes, and desquamation: an ultrastructural study of adult pig epidermis. *Arch Dermatol Res* 282:304–310, 1990
- Elias PM: Lipids and the epidermal permeability barrier. *Arch Dermatol Res* 270:95–117, 1981
- Elias PM, Menon GK: Structural and lipid biochemical correlates of the epidermal permeability barrier. In: Elias P, Havel R, Small D, eds. *Advances in lipid research, V. 24, skin lipids*. San Diego: Academic Press, 1991, p. 1–26
- Elias PM, Menon GK, Grayson S, Brown BE: Membrane structural alterations in murine stratum corneum. Relationship to the localization of polar lipids and phospholipases. *J Invest Dermatol* 91:3–10, 1988
- Fartasch M, Bassukas ID, Diepgen TL: Structural relationship between epidermal lipid lamellae, lamellar bodies and desmosomes in human epidermis: An ultrastructural study. *Br J Dermatol* 128:1–9, 1993
- Forslind B: A domain mosaic model of the skin barrier. *Acta Derm Venerol* 74:1–6, 1994
- Fritsch WC, Stoughton RB: The effect of temperature and humidity on the penetration of C<sup>14</sup> acetylsalicylic acid in excised human skin. *J Invest Dermatol* 41:307–310, 1963
- Grubauer G, Feingold KR, Harris RM, Elias PM: Lipid content and lipid type as determinants of the epidermal permeability barrier. *J Lipid Res* 30:89–96, 1989
- van Hal DA, Jeremiasse E, Junginger HE, Spies F, Bouwstra JA: Structure of fully hydrated human stratum corneum: a freeze-fracture electron microscopy study. *J Invest Dermatol* 106:89–95, 1996
- Halkier-Sørensen L, Petersen BH, Thestrup-Pedersen K: Epidemiology of occupational skin diseases in Denmark: notification, recognition and compensation. In: van der Valk PGM, Maibach HI (eds). *The Irritant Contact Dermatitis Syndrome*. Boca Raton, FL: CRC Press, 1995: pp 23–52
- Hashimoto-Kumasaka K, Horii I, Tagami H: In vitro comparison of water-holding capacity of the superficial and deeper layers of the stratum corneum. *Arch Dermatol Res* 283:342–346, 1991
- Hou SYE, Mitra AK, White SH, Menon GK, Ghadially R, Elias PM: Membrane structures in normal and essential fatty acid-deficient stratum corneum: characterization by ruthenium tetroxide staining and x-ray diffraction. *J Invest Dermatol* 96:215–223, 1991
- Hurkmans JFGM, Boddé HE, Van Driel LMJ, Van Doorne H, Junginger HE: Skin irritation caused by transdermal drug delivery systems during long-term (5 days) application. *Br J Dermatol* 112:461–467, 1985
- Jiang SJ, Hwang SM, Choi EH, Elias PM, Ahn SK, Lee SH: Structural and functional effects of oleic acid and iontophoresis on hairless mouse stratum corneum. *J Invest Dermatol* 114:64–70, 2000
- Johnson ME, Blankstein D, Langer R: Evaluation of solute permeation through the stratum corneum: lateral bilayer diffusion as the primary transport mechanism. *J Pharm Sci* 86:1162–1172, 1997
- Jolly M, Swan AG: The effects on rat skin of prolonged exposure to water. *Br J Dermatol* 103:387–395, 1980
- Kligman AM: Hydration injury to human skin. In: Elsner P, Berardesca E, Maibach HI (eds). *Bioengineering of the Skin: Water and the Stratum Corneum*. Boca Raton, FL: CRC Press, 1994: pp 251–255

- Koyama J, Nakanishi J, Masuda Y, Sato J, Nomura J, Suzuki Y, Nakayama Y: The mechanism of desquamation in the stratum corneum and its relevance to skin care. Skin: interface of a living system (Shiseido Science Symposium '97, Tokyo), New York: Elsevier 1998, 85–94
- Lampe MA, Williams ML, Elias PM: Human epidermal lipids. characterization and modulations during differentiation. *J Lipid Res* 24:131–140, 1983
- Law S, Wertz PW, Swartzendruber DC, Squier CA: Regional variation in content, composition and organization of porcine epithelial barrier lipids revealed by thin-layer chromatography and transmission electron microscopy. *Arch Oral Biol* 40:1085–1091, 1995
- Lindberg M, Forslind B: The effects of occlusion of the skin on the Langerhans cell and the epidermal mononuclear cells. *Acta Derm Venereol (Stockh)* 61:201–205, 1981
- Lindberg M, Johannesson A, Forslind B: The effect of occlusive treatment on human skin: an electron microscopic study on epidermal morphology as affected by occlusion and dansyl chloride. *Acta Derm Venereol (Stockh)* 62:1–5, 1982
- Madison KC, Swartzendruber DC, Wertz PW, Downing DT: Presence of intact intercellular lipid lamellae in the upper layers of the stratum corneum. *J Invest Dermatol* 88:714–718, 1987
- Matoltsy AG, Downes AM, Sweeney TM: Studies of the epidermal water barrier. II. Investigation of the chemical nature of the water barrier. *J Invest Dermatol* 50:19–26, 1968
- Meding B: Differences between the sexes with regard to work-related skin disease. *Contact Dermatitis* 43:65–71, 2000
- Menon GK, Elias PM: Morphologic basis for a pore-pathway in mammalian stratum corneum. *Skin Pharmacol* 10:235–246, 1997
- Menon GK, Grayson S, Brown BE, Elias PM: Lipokeratinocytes of the epidermis of a cetacean (*Phocena phocena*); histochemistry, ultrastructure, and lipid composition. *Cell Tissue Res* 244:385–394, 1986
- Michaels AS, Chandrasekaran SK, Shaw JE: Drug permeation through human skin. Theory and in vitro experimental measurement. *Am Chem Eng J* 21:985–996, 1975
- Mikulowska A: Reactive changes in human epidermis following simple occlusion with water. *Contact Dermatitis* 26:224–227, 1992
- Mikulowska A: Reactive changes in the Langerhans cells of human skin caused by occlusion with water and sodium lauryl sulphate. *Acta Derm Venereol (Stockh)* 70:468–473, 1990
- Norlén L, Emilson A, Forslind B: Stratum corneum swelling. Biophysical and computer assisted quantitative assessments. *Arch Dermatol Res* 289:506–513, 1997
- Onken HD, Moyer CA: The water barrier in human epidermis. *Arch Dermatol* 87:584–590, 1963
- Possick PA: Contact dermatitis. *Cutis* 5:167–170, 1969
- Potts RO, Francoeur ML: The influence of stratum corneum morphology on water permeability. *J Invest Dermatol* 96:495–499, 1991
- Rawlings AV, Harding CR, Watkinson A, Banks J, Ackerman C, Sabin R: The effect of glycerol and humidity on desmosome degradation in stratum corneum. *Arch Dermatol Res* 287:457–464, 1995
- Renshaw B: Observations on the role of water in the susceptibility of human skin to injury by vesicant vapors. *J Invest Dermatol* 9:75–85, 1947
- Rougier A, Dupuis D, Lotte C, Roguet R: Measurement of the stratum corneum reservoir; a predictive method for in vivo percutaneous absorption studies: influence of application time. *J Invest Dermatol* 84:66–68, 1985
- Scheuplein R: Site variations in diffusion and permeability. In: Jarrett A (ed). *The Physiology and Pathophysiology of the Skin*. London: Academic Press, 1978: pp 1731–1752
- Scheuplein RJ, Morgan LJ: “Bound water” in keratin membranes measured by a microbalance technique. *Nature* 214:456–458, 1967
- Scott IR, Harding CR, Barrett JB: Histidine-rich protein of the keratohyalin granules: source of the free amino acids, urocanic acid and pyrrolidone carboxylic acid in mammalian stratum corneum. *Biochim Biophys Acta* 719:110–117, 1982
- Spencer TS, Linamen CE, Akers WA, Jones HE: Temperature dependence of water content of stratum corneum. *Br J Dermatol* 93:159–164, 1975
- Squier CA, Wertz PW, Cox P: Thin-layer chromatographic analyses of lipids in different layers of porcine epidermis and oral epithelium. *Arch Oral Biol* 36: 647–653, 1991
- Steven AC, Bisher ME, Roop DR, Steinert PM: Biosynthetic pathways of filaggrin and lorincrin—two major proteins expressed by terminally differentiated epidermal keratinocytes. *J Struct Biol* 104:150–162, 1990
- Suskind RR, Ishihara M: The effects of wetting on cutaneous vulnerability. *Arch Environ Health* 11:529–537, 1965
- Taplin D, Zaia N, Blank H: The role of temperature in tropical immersion foot syndrome. *JAMA* 202:210–213, 1967
- Vickers CFH: Existence of a reservoir in the stratum corneum. *Arch Dermatol* 88: 20–23, 1963
- Warner RR, Lilly NA: Correlation of water content with ultrastructure in the stratum corneum. In: Elsner P, Berardesca E, Maibach HI (eds). *Bioengineering of the Skin: Water and the Stratum Corneum*. Boca Raton, FL: CRC Press, 1994: pp 3–12
- Warner RR, Bush RD, Ruebusch NA: Corneocytes undergo systematic changes in element concentrations across the human inner stratum corneum. *J Invest Dermatol* 104:530–536, 1995
- Warner RR, Boissy YL, Lilly NA, Spears MJ, McKillop K, Marshall JL, Stone KJ: Water disrupts stratum corneum lipid lamellae: damage is similar to surfactants. *J Invest Dermatol* 113:960–966, 1999
- Willis I: The effects of prolonged water exposure on human skin. *J Invest Dermatol* 60:166–171, 1973
- Zhai H, Ebel JP, Chatterjee R, et al Hydration versus skin permeability to nicotines in man. *Skin Res Technol* 2001, 8:13–18, 2002
- Zimmerer RE, Lawson KD, Calvert CJ: The effects of wearing diapers on skin. *Pediatr Dermatol* 3:95–101, 1986